



## A true oxygen-linked heptazine based polymer for efficient hydrogen evolution



V.R. Battula<sup>1</sup>, Sunil Kumar<sup>1</sup>, D.K. Chauhan, Soumadri Samanta, Kamalakannan Kailasam\*

*Institute of Nano Science and Technology (INST), Phase 10, SAS Nagar, Mohali 160062, India*

### ARTICLE INFO

**Keywords:**

Water splitting  
Heterogeneous photocatalysis  
Heptazine  
Carbon nitride  
Cyameluric acid

### ABSTRACT

O-doped/functional g-CN polymers are promising materials which have been reported to modify inherent electronic structure and light harvest ability of the g-C<sub>3</sub>N<sub>4</sub> based photocatalysts. However, the doping position and concentration of hetero atom remains ill-defined although enhanced photocatalytic activity of modified g-CN photocatalysts has been reported. Herein, a facile two step procedure to synthesize heptazine polymer with defined O-atom position in polymer structure is presented. Cyameluric acid, a member of cyamelurine family upon polycondensation under inert atmosphere ensures the insertion of O-atom at bridge position between heptazine units in growing polymer. The developed polymer OLHP (oxygen linked heptazine polymer) attains high hydrogen production efficiency likely due to high O-content and efficient charge separation evident from PL spectra compared to g-CN. This heptazine based precursor design also eliminates the possibility of presence of triazine based moiety defects in g-C<sub>3</sub>N<sub>4</sub> polymers.

### 1. Introduction

Driving the global energy system into a sustainable path is progressively becoming a major concern and worldwide policy objective. Ever since, the production of hydrogen is at the centre of intensive research initiatives among the researchers. Artificial photosynthesis is a green, safe and inexpensive process utilizing the vastly available sunlight and water as energy source and raw material, respectively, for molecular hydrogen production. Since Fujishima and Honda reported water splitting using TiO<sub>2</sub> in 1972 [1], inorganic and then organic/polymeric photoactive semiconductors have been developed and their hydrogen evolution performance was studied. Although, inorganic semiconductors are stable but the shortcoming of band gap tuning due to the material processing difficulties, the deemed photocatalysis is yet to be achieved [2]. Moreover, the organic/polymeric semiconductors gained interest of scientific community when breakthrough research article describing the splitting of water to molecular hydrogen on polymeric carbon nitride, g-CN (generally called as g-C<sub>3</sub>N<sub>4</sub>) in the presence of sacrificial reagents was reported in the year 2009 [3]. g-C<sub>3</sub>N<sub>4</sub> possess ideal semiconductor photocatalyst properties such as band position, thermal stability, efficiency and robustness for water splitting to produce hydrogen. Its easy preparation from urea or melamine like cheap precursors also adds to the low cost synthesis feature to its large

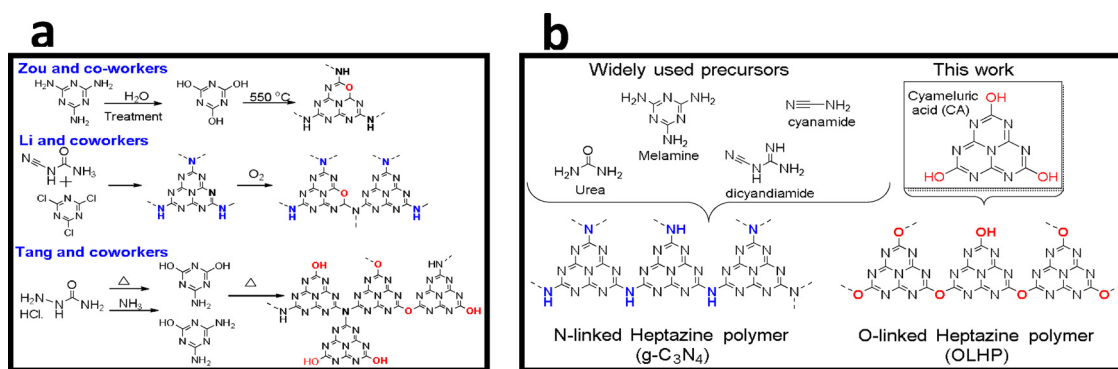
scale production [4]. However, due to the relatively large band gap, dense π-π stacking and fast charge recombination, current performance of g-C<sub>3</sub>N<sub>4</sub> is only moderate [5]. In order to improve the band gap and slower the charge recombination rate on catalyst surface, elemental doping, quantum dot sensitization, heterojunction, organic functionalization, nitrogen defects/vacancy were introduced, and modified precursors have been used in g-C<sub>3</sub>N<sub>4</sub> synthesis to enhance the photocatalytic performance of g-C<sub>3</sub>N<sub>4</sub> and the developed material have been used for various applications [6–27].

Among all the methods to improve the properties of g-CN, elemental doping is widely used by researchers. Especially non-metal doping (B, C, O, F, P and S) have established their key role in enhancing the sunlight absorption by catalyst and its photoactivity [28–48]. Out of these, O-doping has shown significant enhancement in the photocatalytic activity by improving the electronic band structure and charge carrier utilization. Scheme 1a provides examples of some strategies to introduce O-atom into the g-CN structure. Many of the reports claim that the incorporation of O-containing functionalities into the g-C<sub>3</sub>N<sub>4</sub> enhance the visible light absorption and photocatalytic activity [33,49,50]. O-doped g-CN is easily synthesized by treating its precursor melamine with H<sub>2</sub>O<sub>2</sub> or by treating g-CN with H<sub>2</sub>O<sub>2</sub> or under oxygen atmosphere [51–53]. But, the control over the position of O-atom in the final structure is difficult which causes different consequences for the

\* Corresponding author.

E-mail address: [kamal@inst.ac.in](mailto:kamal@inst.ac.in) (K. Kailasam).

<sup>1</sup> Authors contributed equally.



**Scheme 1.** (a) Some of reported strategies to introduce O-atom into the g-CN structure, and (b) Overview of the previous precursors used in g-C<sub>3</sub>N<sub>4</sub> synthesis and the precursor used in this work to synthesize heptazine polymer (OLHP).

photophysical and chemical properties, although the increment in photocatalytic activity has been observed. Moreover, one can question the reproducibility of modified photocatalyst structure to be considered for practical applications.

Oxygen-modified monolayer g-C<sub>3</sub>N<sub>4</sub> was reported using thermal oxidation method which were highly crystalline and attained external quantum efficiency (EQE) of 13.7% (at 420 nm) for H<sub>2</sub> evolution from the synthesized nanosheets [54]. Fan et al. reported porous and simultaneously highly ordered O-doped carbon nitride prepared from hydrothermally treated dicyandiamide to introduce O-functionality in precursor design [55]. Zou et al. also reported 11.3 times higher hydrogen evolution by developing O-doped bulk g-C<sub>3</sub>N<sub>4</sub> from melamine which was modified hydrothermally to obtain a hydrogen bonded supramolecular complex as precursor [56]. Li et al. recently reported a procedure for oxygen self-doping of carbon nitride and reported 4-times higher H<sub>2</sub> evolution under visible light for the modified catalyst compared to bulk carbon nitride [57]. The reported precursor design involved the premixing of 1,3,5-trichlorotriazine with variable amounts of dicyandiamide in acetonitrile and then autoclaving the mixture at 200 °C for 24 h. Unlike other reports, the procedure did not use specific doping protocol and the assessed O-doping was only the result of precursor design. Moreover, the proposed pathways to tune the band gap and electronic levels of catalyst do not always boost up the photocatalytic efficiency. In a very recent report from Tang et al., theoretical models facilitated the rational designing of oxygen and nitrogen linked heptazine polymer (ONLH) which resulted in band gap narrowing and benchmark 25 times higher H<sub>2</sub> evolution ( $\lambda > 420$  nm) than g-C<sub>3</sub>N<sub>4</sub> [58]. Based on this knowledge, we understand that the chemical structure modifications leading to the covalent insertion of O-atom into the g-CN should be interesting for photocatalyst material design. Moreover, if the desired atom-modifications are position specific, regular and reproducible, then we believe that such precursor designing will be able to solve the problems related to ambiguous doping concentration and position of incorporated element in the final polymer structure. Thus, designing precursors is a more precise way to introduce desired element covalently as part of the chemical structure of photocatalysts.

In this context, novel heptazine based polymers were developed where the O-atom was inserted as linker atom between adjacent heptazine units in the polymer. Cyameluric acid (CA), a member of cyamelurine was used as the precursor because upon polycondensation, only oxygen will be incorporated as linking atom between heptazine units of the growing polymer. This approach would favour the formation of oxygen linked heptazine polymer (should not be confused with O-doped g-CN) which makes it different from g-CN where  $-\text{NH}_x$  is the bridging unit (refer Scheme 1b).

Heptazine based monomers (except 2,5,8-Triazido-s-Heptazine) [59] has rarely been utilized for the synthesis of g-C<sub>3</sub>N<sub>4</sub> and thus we consider that, to the best of our knowledge, this is the first report of true

O-linked heptazine polymer developed using heptazine based precursor. In addition to uncertainty in doping (position and concentration), this heptazine precursor leads only to heptazine based polymer unlike in g-CN where incomplete cyclization and impurities from precursors has also been considered to be the part of final structure [60]. This is due to the use of alicyclic or triazine based molecular compounds shown in Scheme 1b for the synthesis of g-C<sub>3</sub>N<sub>4</sub>. Moreover, the effect of O-linkage on photophysical and photoactivity was studied in comparison to g-CN-550 developed under similar conditions. This strategy of heptazine based rational precursor design gives a new member to the Carbon nitride family with controlled doping of heteroatoms into polymer with better reproducibility of photocatalyst for applying them in emerging applications.

## 2. Results and discussions

The oxygen linked Heptazine based polymer (OLHP) has been synthesized by simple thermal polymerization of Cyameluric acid (CA) at different temperatures and for comparison purpose the g-CN was also synthesized along with OLHP. The detailed synthesis procedure is given supporting information. The crystal structures of OLHP-550, OLHP-450 and g-CN-550 were compared by using Powder X-Ray Diffraction (PXRD) as shown in Fig. 1a g-CN-550 exhibits diffraction peak at 27.4° and 13.1° which are characteristic peaks for the layered stack of conjugated heptazine units (with interlayer distance, 0.32 nm) and in-plane repeating heptazine units, respectively [56,58]. The similar XRD signature was observed for synthesized OLHPs signifying layered heptazine polymers. The intense diffraction peak for OLHP-550 and OLHP-450 shifted toward lower angles, 27.1° for both polymers compared to g-CN which proved increase in distance of interlayer stacking in OLHP layers. The broad diffraction peaks for OLHPs compared to g-CN signified the distortion from planarity in grown polymers [58]. Thermal stability study of cyameluric acid carried out in N<sub>2</sub> atmosphere provides understanding of the polymerization process of precursor and OLHP-550 (Fig. S1). Cyameluric acid shows two step mass loss between 270 to 450 °C and 470 to 600 °C. Thus, the precursor polymerisation will take place effectively between 450 and 550 °C as the precursor decomposes at 600 °C. Further, the TGA curve of OLHP-550 shows a small mass loss of 7% between 310–365 °C and then major mass loss occurred after 437 °C up to complete mass loss at 600 °C (Fig. S1). The mass loss at 310 °C could be related to the presence of oligomeric/smaller chains of polymer during the formation of OLHP-550. The N<sub>2</sub> physisorption measurements revealed the BET surface area of 11.3, 10.4 and 15.9 m<sup>2</sup>/g for OLHP-550, OLHP-450 and g-CN-550, respectively (Fig. 1b). There is no significant change in the surface area as both these polymers were synthesized using high temperature process without any templates. Fig. 1c shows the DRUV-vis spectra for OLHP-550, OLHP-450 and g-CN-550 and both showed similar absorption behaviour to g-CN-550 with slight shift of absorption onset toward longer wavelength. The band gap

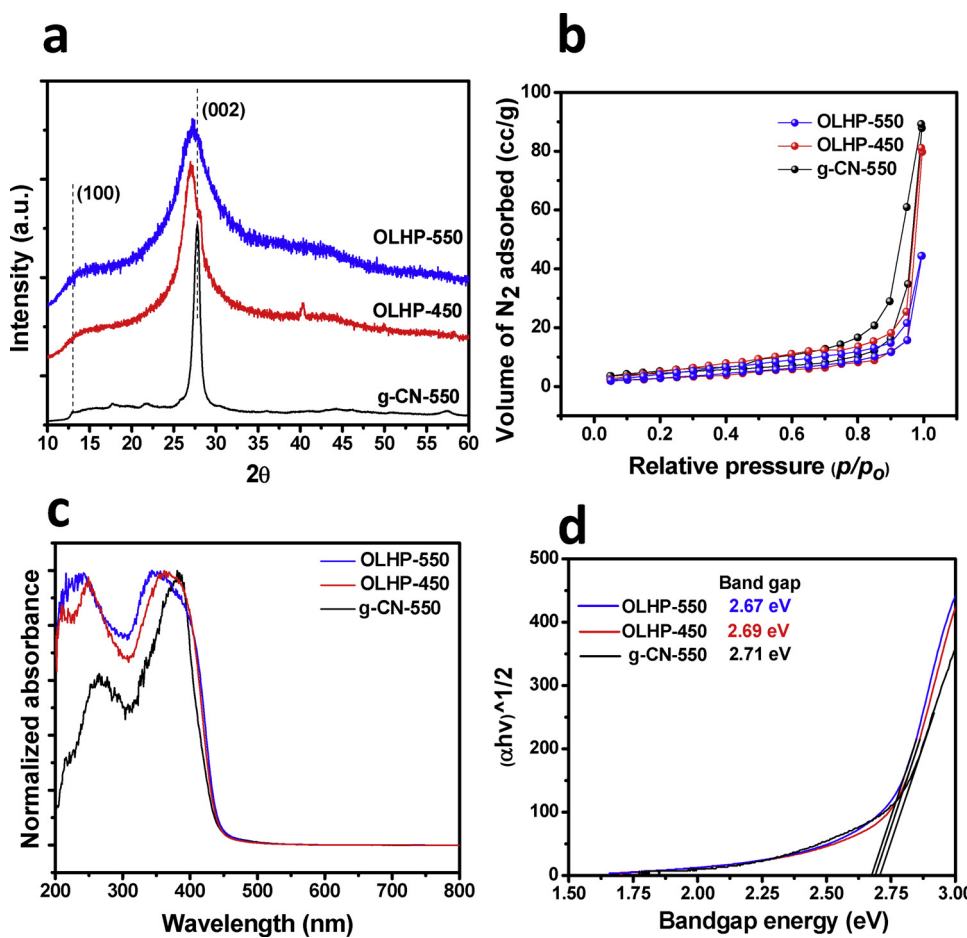


**Fig. 1.** (a) Powder XRD pattern and (b)  $N_2$  physisorption isotherms for, (c) DRUV-Vis spectra and d) Tauc plot of OLHP-550, OLHP-450 and g-CN-550.

energies were estimated from the corresponding Tauc plots as shown in Fig. 1d. The band gap for OLHP-550 and OLHP-450 were calculated to be 2.67 and 2.69 eV, respectively, in comparison to 2.71 eV for the as-synthesized g-CN-550. There is slight decrease in band gaps with wider absorption for OLHP-550 and OLHP-450 compared to g-CN-550.

Infrared spectroscopy (IR) provides the structural information and clearly depicts the formation of OLHP-550 (Fig. S2). The peak at  $804\text{ cm}^{-1}$  represents the breathing mode of heptazine system in both OLHPs and g-CN-550. The IR peaks for OLHP-550 in  $1100\text{--}1500\text{ cm}^{-1}$  region are less intense than the peaks of g-CN-550, as expected for the increased number of C–O bonds in OLHP-550 than g-CN-550. Finally, in the region  $3000\text{--}3400\text{ cm}^{-1}$  for g-CN-550 shows the broad curve representing  $\text{NH}_x$  peaks. While in OLHP-550, the peak in the same region becomes less broad and less intense which corresponds to the presence of terminal hydroxyl units. The charge carrier recombination process in OLHPs and g-CN-550 were compared using photoluminescence (PL) studies (Fig. 2). The intense PL emission maximum was observed around  $470\text{ nm}$  for g-CN-550 and OLHPs ( $\lambda_{\text{exc}} = 370\text{ nm}$ ). But the intensity of the emission decreased in the order  $\text{OLHP-450} > \text{OLHP-550}$ . The intense PL emission for g-CN-550 signifies the significant recombination of the electrons and holes which is detrimental for the photocatalytic activity. Whereas in OLHP-550, PL intensity is decreased which indicates that the O-bridged (linked) heptazines have enhanced electron-hole separation due to their slow recombination which enhancing the photocatalytic activity of OLHP-550 [58,61]. To ensure this, electrochemical impedance spectroscopy (EIS) Nyquist plot was studied. It was observed that the arc radius of the OLHP-550 catalyst was smaller than g-CN-550 (Fig. S3a). This decreased arc radius indicates more effective separation of photo-generated electron-hole pairs and faster interfacial charge transfer on

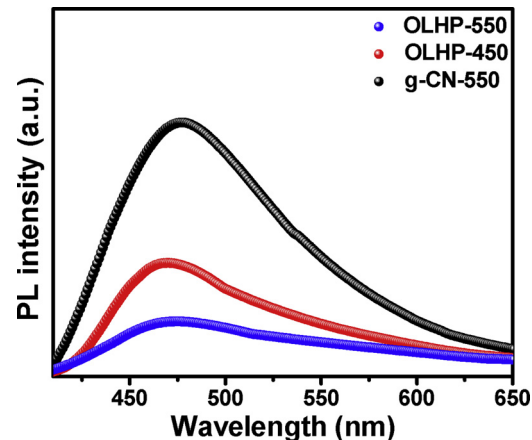


**Fig. 2.** Solid PL spectra of OLHP-550, OLHP-450, g-CN-550 ( $\lambda_{\text{exc}} = 370\text{ nm}$ ).

the catalyst surface in OLHP-550 [62]. Further, the effect of bridged oxygen has been shown in photocurrent responses (Fig. S3b). The enhancement of photocurrent of OLHP-550 to that of g-CN-550 indicates the improved charge separation in OLHP-550 due to bridged oxygen. Therefore, the above DRUV-Vis, PL, EIS, and Photocurrent studies clearly reveal the exact role of oxygen on optical properties of OLHP-550. The oxygen at bridged position has no significant effect on light absorption but absolutely enhances the charge separation, which may improve its photocatalytic activity.

X-ray photoelectron spectroscopy (XPS) was conducted to verify the chemical states of elements present and verify that the oxygen is

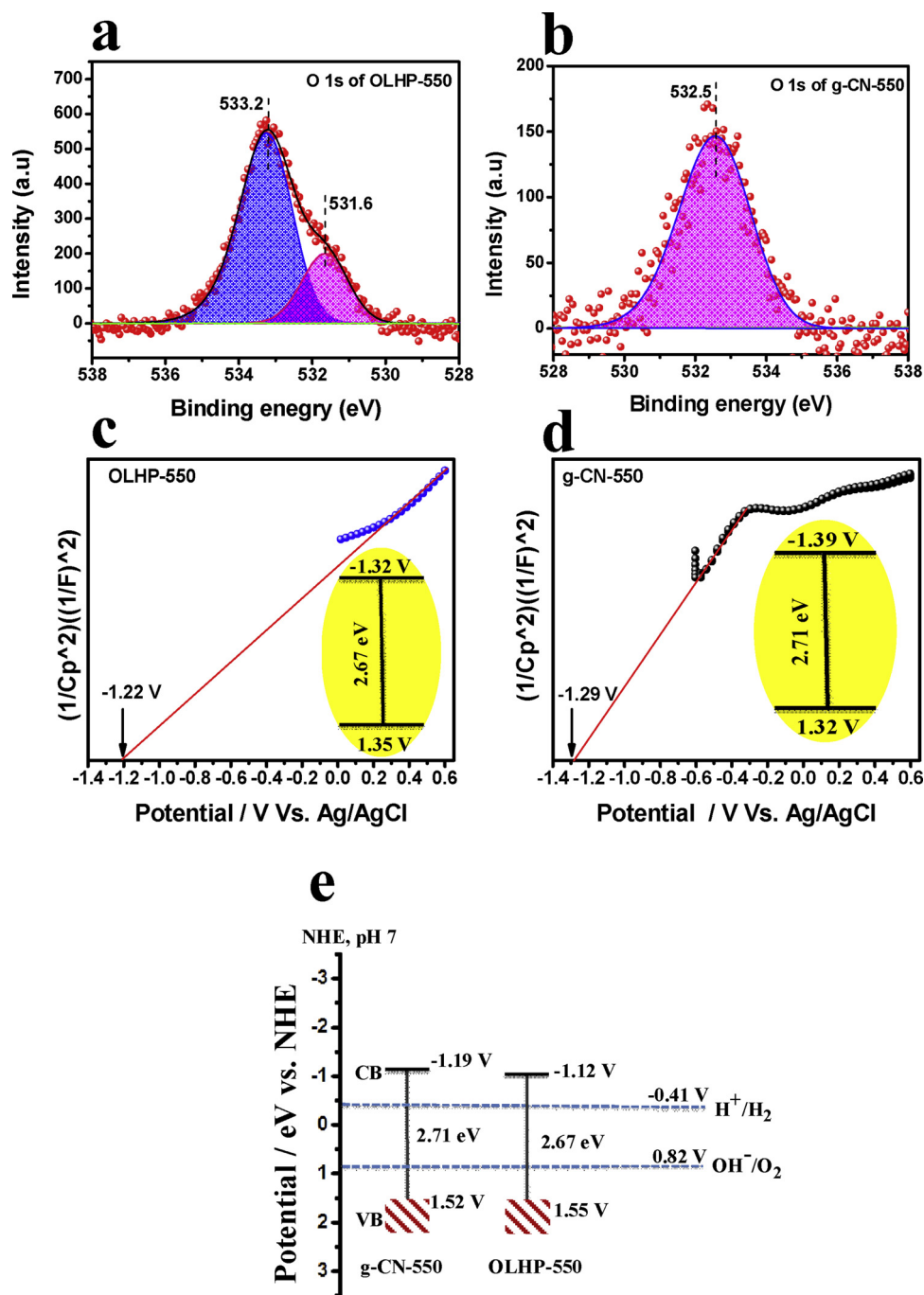


**Fig. 3.** (a) O1s XPS spectra of OLHP-550, (b) O1s XPS spectra of g-CN-550, (c) Mott-Schottky plot for OLHP-550, (d) Mott-Schottky plot for g-CN-550, and (e) band diagram of OLHP-550 and g-CN.

present at bridge position in the oxygen linked heptazine based polymers. Consistent from the expected structure of OLHP-550 as depicted in Fig. 3, an increase in the percentage of O1s peak is observed while the N1s peak is found to be less intense for OLHP-550 as compared to g-CN-550 (Figs. S4 and S5). These results indicate that the OLHP has higher quantity of O-atoms [58]. The O1s spectra of OLHP-550 (Fig. 3a) displays two new peaks corresponding to C–OH and C–O–C species are observed at 531.6 and 533.2 eV, respectively. The C–O–C peak confirms the presence of O-atom as bridge between adjacent heptazine units in polymer network while C–OH peak corresponds to the terminal hydroxyl groups remained at the edges of polymer. While O1s spectra of g-CN-550 displays a very weak peak at 532.5 eV which may due to adsorbed moisture (Fig. 3b). The C1s spectra of both

samples (Fig. S6) exhibits intense peak at 288 eV and could easily be assigned to N=C–N ( $sp^2$  hybridised carbon) species in the heptazine unit. The other peak at 286.2 eV in g-CN-550 is very weak and could arise due to the contaminating amount of oxygen in polymer structure. But, the intensity of same peak was strong for OLHP-550 (286.5 eV) which also indicated the presence of more C–O bonds than in g-CN. The N1s spectra of g-CN-550 (Fig. S6) resembles to the typical peaks for N-linked heptazine polymer (g-CN) confirming the presence of C=N–C (398 eV), N-(C)<sub>3</sub> (399.5 eV), –NH<sub>x</sub> (401 eV) and C=N (404.4 eV) in aromatic CN heterocycle, respectively. However, similar peaks were present in OLHP-550 at 398.9 eV, 400.3 eV and 404.4 eV except the peak for –NH<sub>x</sub> been not observed which proves the absence of –NH<sub>x</sub> bridge in OLHP-550 and had been replaced with O-bridges. Moreover,

**Table 1**

Investigation of Photocatalytic H<sub>2</sub> evolution by using OLHP compounds under visible light at room temperature.

Entry	Catalyst <sup>a</sup>	Pt (Wt. %)	Water (mL)	TEOA (mL)	H <sub>2</sub> (μL)
1	–	–	10	–	(n.d.)
2	10 mg	–	10	–	n.d.
3	10 mg	–	9	1	n.d.
4	10 mg	3	10	–	n.d.
5	10 mg	3	9	1	227
6	10 mg	3	9	1 <sup>b</sup>	207
7	10 mg	3	9	1 <sup>c</sup>	49
8	50 mg	3	18	2	1223

n.d. = not detected within GC detection limit.

<sup>a</sup> Reaction conditions: Catalyst = OLHP-550, LED solar simulator (> 400 nm, 150 mW cm<sup>-2</sup>), Reaction time = 6 h. Co-catalyst = 3 wt % Pt, Sacrificial agent = Triethanolamine (TEOA).

<sup>b</sup> Methanol.

<sup>c</sup> Isopropyl alcohol.

no other changes in the heptazine unit of OLHPs was observed in XPS spectra which emphasizes the development of a true O-linked heptazine polymer by choosing cyameluric acid as precursor [58,62]. Moreover, the presence of excess oxygen percentage in OLHP samples has been further supported by the elemental mapping as shown in Fig. S7. Further, the TEM images of OLHP-550 reveals similar type of layered morphology to that of g-CN-550 (Fig. S8). To identify the possible band positions (valence and conduction band), Mott-Schottky measurements were carried out (Fig. 3c). The positive slope suggested n-type semiconductor and corresponding conduction band minima (CBM) was estimated as –1.32 V Vs. Ag/AgCl from the obtained flat band potential (–1.22 V) since for most of the n-type semiconductors the flat band potential lies 0.1 V below the CBM [63]. Optical band gap was used further to locate the valence band maximum (VBM) as 1.35 V Vs. Ag/AgCl for the OLHP-550 as shown in the inset of Fig. 3c. Similarly, we estimated the band positions of g-CN-550 as shown in Fig. 3d. The band positions with respect to NHE are provided in Fig. 3e which clearly shows that OLHP-550 energetically favours the hydrogen evolution.

### 3. Photocatalytic activity

After critical examination of the catalyst, its photocatalytic activity was investigated in terms of H<sub>2</sub> evolution by water splitting under visible light (> 400 nm) by using triethanolamine (TEOA) as electron donor and Pt as co-catalyst as mentioned in Table 1. The initial 5 experiments in Table 1 confirmed the necessity of all components for H<sub>2</sub> evolution under visible light. No H<sub>2</sub> was detected within the detection limit of GC in case of experiments without Pt and TEOA (Entry 2 in Table 1), without Pt and with TEOA (Entry 3 in Table 1), with Pt and without TEOA (Entry 4 in Table 1). Higher amount of H<sub>2</sub> was detected

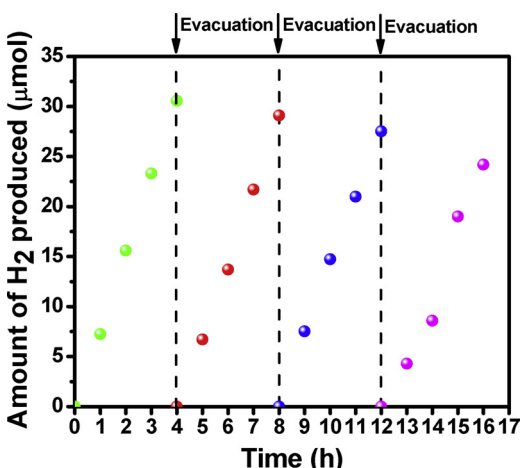


Fig. 5. Stability cycles for H<sub>2</sub> evolution for 16 h with OLHP-550 (3 wt% Pt). Reaction conditions: 50 mg catalyst, 20 mL water (10 vol % TEOA). Light source: LED solar simulator (> 400 nm, 150 mW cm<sup>-2</sup>).

in GC in case of TEOA (Entry 5 in Table 1) compared to Methanol and IPA (Entry 6 and 7 in Table 1). Further, on increasing the catalyst loading and volume of water (10% TEOA), we observed a drastic increase in the amount of H<sub>2</sub> produced (Entry 8 in Table 1).

Experiments were carried out on g-CN-550 to compare and investigate the effect of O-linkage on the photocatalytic activity compared to the N/NH<sub>x</sub> linkage in g-CN (Fig. 4a). The hydrogen evolution rate produced by using OLHP-550 was about 8.75 μmol/h which is 41 times higher compared to g-CN-550 (0.216 μmol/h). In case of OLHP-450, it was only about 0.875 μmol/h. The reason for the superior activity of OLHP-550 over g-CN-550 and OLHP-450 could be due to its completely polymerized heptazine structure, optimum band gap and slower charge recombination as evident from the PL spectra (Fig. 2). Further, we decided to check the H<sub>2</sub> evolution ability of OLHP-550 under natural sunlight rather than using artificial sunlight (requires lots of expenditure which is detrimental for practicality/commercialization) to mimic artificial photosynthesis. The reactions were performed under natural sunlight (March 17th, 2018) for 7.5 h from 10:30 AM until 6:00 PM. The OLHP-550 produced a significant amount of H<sub>2</sub> (272 μL) after 7.5 h of reaction time under natural sunlight (Fig. 4b) in comparison by using solar simulator which produced 390 μL of H<sub>2</sub> after 7.5 h. From the above results, OLHP-550 shows a more promising candidate for H<sub>2</sub> production than g-CN. Thus, the oxygen linkage between Heptazine units in OLHP rather than N/NH<sub>x</sub> linkage had showed a dramatic improvement in photocatalytic H<sub>2</sub> evolution. Thus, further organic modification and subsequent introduction of nanoporosity could increase the H<sub>2</sub> evolution in these OLHPs and can pave way for new heptazine polymers for further scrutinization in various

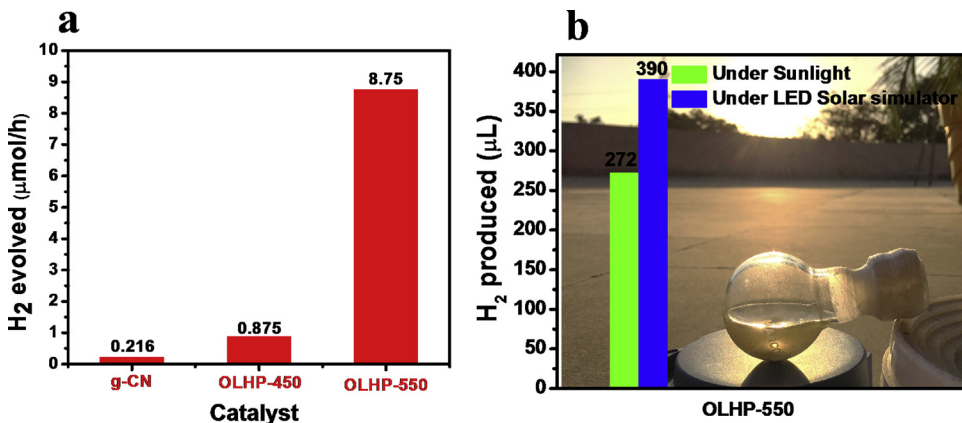


Fig. 4. (a) Comparison of HER of g-CN, OLHP-450 and OLHP-550. Reaction conditions: 50 mg catalyst, reaction time of 6 h, Pt (3 wt%) as co-catalyst and TEOA as sacrificial electron donor. Light source = LED solar simulator (> 400 nm, 150 mW cm<sup>-2</sup>). (b) H<sub>2</sub> produced under sunlight (76 mW cm<sup>-2</sup>) and LED solar simulator (> 400 nm, 150 mW cm<sup>-2</sup>). Reaction conditions: 10 mg OLHP-550, reaction time of 7.5 h, Pt (3 wt%) as co-catalyst and TEOA as sacrificial electron donor.

applications.

In order to investigate the robustness and stability of as synthesized OLHP-550, we performed a 16 h cycle experiment with OLHP-550 (3 wt % Pt). The reaction system was re-evacuated and purged with N<sub>2</sub> for every 4 h during the reaction. The activity of OLHP-550 was maintained even after 16 h (Fig. 5). It produced a total of 111 μmol of H<sub>2</sub> after 16 h. To note that the H<sub>2</sub> evolution was slightly decreased from first cycle to fourth cycle and it might be due to the decrease in the amount of TEOA after each cycle. Further, FT-IR spectra of OLHP-550 was recorded after 4 cycles, which proved that there was no change in structure of OLHP-550 (Fig. S9).

#### 4. Conclusion

In summary, we have successfully synthesized a true oxygen linked Heptazine polymers (OLHP) by introducing cyameluric acid (CA) as a new precursor. This precursor not only introduces the new heptazine polymer containing O-bridges unlike g-CN which is NH<sub>x</sub>-bridged heptazine polymer but also paves the path to explore new precursors for noble heptazine polymers. The PXRD patterns proves similar graphitic nature of OLHP-550 to the parent g-CN. The FTIR given the initial insights of O-linkage in OLHP-550 which was further confirmed by the XPS analysis. We have successfully demonstrated the effect of O-linkage on the optical properties/band structure of OLHP-550. The O-linkage improved the hydrogen evolution rate of OLHP-550 by 41 folds higher than that of g-CN. This study may attract researchers towards various heptazine based precursors for the synthesis of only heptazine based polymers with defined hetero atom in the polymer structure. Also it will provide the right precursor selection which holds the key to solve the problem of reproducibility of the polymeric structures.

#### Competing financial interests

Authors declare no competing financial interests.

#### Acknowledgments

Dr Kamalakannan Kailasam thanks DST-Nano Mission NATDP funded Technology Project, File No. SR/NM/NT-06/2016 and DST-SERB for the Early Career Research Award (ECR), File No. ECR/2016/001469. Dr Sunil Kumar is thankful to SERB for NPDF fellowship (PDF/2016/002227) for the financial support. V.R. Battula and Soumadri Samanta thank INST Mohali for funding.

#### Appendix A. Supplementary data

Supplementary material related to this article can be found, in the online version, at doi:<https://doi.org/10.1016/j.apcatb.2018.11.027>.

#### References

- [1] A. Fujishima, K. Honda, Electrochemical photolysis of water at a semiconductor electrode, *Nature* 238 (1972) 37.
- [2] D.S. Su, J. Zhang, B. Frank, A. Thomas, X. Wang, J. Paraknowitsch, R. Schlögl, Metal-free heterogeneous catalysis for sustainable chemistry, *ChemSusChem* 3 (2010) 169–180.
- [3] X. Wang, K. Maeda, A. Thomas, K. Takahashi, G. Xin, J.M. Carlsson, K. Domen, M. Antonietti, A metal-free polymeric photocatalyst for hydrogen production from water under visible light, *Nat. Mater.* 8 (2009) 76.
- [4] J. Zhu, P. Xiao, H. Li, S.A.C. Carabineiro, Graphitic carbon nitride: synthesis, properties, and applications in catalysis, *ACS Appl. Mater. Interfaces* 6 (2014) 16449–16465.
- [5] R. Godin, Y. Wang, M.A. Zwijnenburg, J. Tang, J.R. Durrant, Time-resolved spectroscopic investigation of charge trapping in carbon nitrides photocatalysts for hydrogen generation, *J. Am. Chem. Soc.* 139 (2017) 5216–5224.
- [6] Y. Wang, H. Li, J. Yao, X. Wang, M. Antonietti, Synthesis of boron doped polymeric carbon nitride solids and their use as metal-free catalysts for aliphatic C–H bond oxidation, *Chem. Sci.* 2 (2011) 446–450.
- [7] J. Fang, H. Fan, M. Li, C. Long, Nitrogen self-doped graphitic carbon nitride as efficient visible light photocatalyst for hydrogen evolution, *J. Mater. Chem. A* 3 (2015) 13819–13826.
- [8] G. Shien, D. Zhaopeng, L. Mingxia, J. Baojiang, T. Chungui, P. Qingjiang, F. Honggang, phosphorus-doped carbon nitride tubes with a layered micro-nanostructure for enhanced visible-light photocatalytic hydrogen evolution, *Angew. Chem. Int. Ed.* 55 (2016) 1830–1834.
- [9] K. Yuyang, Y. Yongqiang, Y. Li-Chang, K. Xiangdong, L. Gang, C. Hui-Ming, An amorphous carbon nitride photocatalyst with greatly extended visible-light-t-responsive range for photocatalytic hydrogen generation, *Adv. Mater.* 27 (2015) 4572–4577.
- [10] Z. Jinsui, C. Xiufang, T. Kazuhiko, M. Kazuhiko, D. Kazunari, E.J. Dirk, F. Xianzhi, A. Markus, W. Xinchen, Synthesis of a carbon nitride structure for visible-light catalysis by copolymerization, *Angew. Chem. Int. Ed.* 49 (2010) 441–444.
- [11] H. Yu, R. Shi, Y. Zhao, T. Bian, Y. Zhao, C. Zhou, G.I.N. Waterhouse, L.-Z. Wu, C.-H. Tung, T. Zhang, Alkali-assisted synthesis of nitrogen deficient graphitic carbon nitride with tunable band structures for efficient visible-light-driven hydrogen evolution, *Adv. Mater.* 29 (2017) 1605148.
- [12] J. Zhang, M. Zhang, S. Lin, X. Fu, X. Wang, Molecular doping of carbon nitride photocatalysts with tunable bandgap and enhanced activity, *J. Catal.* 310 (2014) 24–30.
- [13] Y. Liu, K. Yan, J. Zhang, Graphitic carbon nitride sensitized with CdS quantum dots for visible-light-driven photoelectrochemical aptasensing of tetracycline, *ACS Appl. Mater. Interfaces* 8 (2016) 28255–28264.
- [14] L. Lu, Z. Lv, Y. Si, M. Liu, S. Zhang, Recent progress on band and surface engineering of graphitic carbon nitride for artificial photosynthesis, *Appl. Surf. Sci.* 462 (2018) 693–712, <https://doi.org/10.1016/j.apsusc.2018.08.131>.
- [15] L. Jiang, X. Yuan, Y. Pan, J. Liang, G. Zeng, Z. Wu, H. Wang, Doping of graphitic carbon nitride for photocatalysis: a review, *Appl. Catal. B* 217 (2017) 388–406.
- [16] B. Kurpil, A. Savateev, V. Papaefthimiou, S. Zafeiratos, T. Heil, S. Özenler, D. Dontsova, M. Antonietti, Hexaazatriphenylene doped carbon nitrides—biomimetic photocatalyst with superior oxidation power, *Appl. Catal. B* 217 (2017) 622–628.
- [17] B. Kurpil, K. Otte, M. Antonietti, A. Savateev, Photooxidation of N-acylhydrazones to 1,3,4-oxadiazoles catalyzed by heterogeneous visible-light-active carbon nitride semiconductor, *Appl. Catal. B* 228 (2018) 97–102.
- [18] X. Wang, X. Chen, A. Thomas, X. Fu, M. Antonietti, Metal-containing carbon nitride compounds: a new functional organic–metal hybrid material, *Adv. Mater.* 21 (2009) 1609–1612.
- [19] H. Ou, X. Chen, L. Lin, Y. Fang, X. Wang, Biomimetic donor–acceptor motifs in conjugated polymers for promoting exciton splitting and charge separation, *Angew. Chem. Int. Ed.* 57 (2018) 8729–8733.
- [20] M. Zhou, Z. Hou, L. Zhang, Y. Liu, Q. Gao, X. Chen, n/n junctioned g-C<sub>3</sub>N<sub>4</sub> for enhanced photocatalytic H<sub>2</sub> generation, *Sustain. Energy Fuels* 1 (2017) 317–323.
- [21] P. Yang, R. Wang, M. Zhou, X. Wang, Photochemical Construction of carbon nitride structures for red-light redox catalysis, *Angew. Chem. Int. Ed.* 57 (2018) 8674–8677.
- [22] X.-J. Sun, D.-D. Yang, H. Dong, X.-B. Meng, J.-L. Sheng, X. Zhang, J.-Z. Wei, F.-M. Zhang, ZIF-derived Co<sup>3+</sup> as a cocatalyst for enhanced photocatalytic H<sub>2</sub> production activity of g-C<sub>3</sub>N<sub>4</sub>, *Sustain. Energy Fuels* 2 (2018) 1356–1361.
- [23] G. Zhang, L. Lin, G. Li, Y. Zhang, A. Savateev, S. Zafeiratos, X. Wang, M. Antonietti, Iono-thermal synthesis of triazine–heptazine-based copolymers with apparent quantum yields of 60 % at 420 nm for solar hydrogen production from “Sea Water”, *Angew. Chem. Int. Ed.* 57 (2018) 9372–9376.
- [24] Y. Chen, G. Jia, Y. Hu, G. Fan, Y.H. Tsang, Z. Li, Z. Zou, Two-dimensional nanomaterials for photocatalytic CO<sub>2</sub> reduction to solar fuels, *Sustain. Energy Fuels* 1 (2017) 1875–1898.
- [25] X. Chen, J. Zhang, X. Fu, M. Antonietti, X. Wang, Fe-g-C<sub>3</sub>N<sub>4</sub>-catalyzed oxidation of benzene to phenol using hydrogen peroxide and visible light, *J. Am. Chem. Soc.* 131 (2009) 11658–11659.
- [26] Y. Cui, Z. Ding, X. Fu, X. Wang, Construction of conjugated carbon nitride nanoarchitectures in solution at low temperatures for photoredox catalysis, *Angew. Chem. Int. Ed.* 51 (2012) 11814–11818.
- [27] J. Yan, P. Li, H. Bian, H. Wu, S. Liu, Synthesis of a nano-sized hybrid C<sub>3</sub>N<sub>4</sub>/TiO<sub>2</sub> sample for enhanced and steady solar energy absorption and utilization, *Sustain. Energy Fuels* 1 (2017) 95–102.
- [28] G. Dong, K. Zhao, L. Zhang, Carbon self-doping induced high electronic conductivity and photoreactivity of g-C<sub>3</sub>N<sub>4</sub>, *Chem. Commun.* 48 (2012) 6178–6180.
- [29] J. Zhang, J. Sun, K. Maeda, K. Domen, P. Liu, M. Antonietti, X. Fu, X. Wang, Sulfur-mediated synthesis of carbon nitride: Band-gap engineering and improved functions for photocatalysis, *Energy Environ. Sci.* 4 (2011) 675–678.
- [30] Y. Zhang, A. Thomas, M. Antonietti, X. Wang, Activation of carbon nitride solids by protonation: morphology changes, enhanced ionic conductivity, and photo-conduction experiments, *J. Am. Chem. Soc.* 131 (2009) 50–51.
- [31] X. Li, A.F. Masters, T. Maschmeyer, Polymeric carbon nitride for solar hydrogen production, *Chem. Commun.* 53 (2017) 7438–7446.
- [32] J. Li, B. Shen, Z. Hong, B. Lin, B. Gao, Y. Chen, A facile approach to synthesize novel oxygen-doped g-C<sub>3</sub>N<sub>4</sub> with superior visible-light photoreactivity, *Chem. Commun.* 48 (2012) 12017–12019.
- [33] Z.-F. Huang, J. Song, L. Pan, Z. Wang, X. Zhang, J.-J. Zou, W. Mi, X. Zhang, L. Wang, Carbon nitride with simultaneous porous network and O-doping for efficient solar-energy-driven hydrogen evolution, *Nano Energy* 12 (2015) 646–656.
- [34] S. Liu, H. Sun, M.H. Ang, M.O. Tade, S. Wang, Integrated oxygen-doping and dye sensitization of graphitic carbon nitride for enhanced visible light photodegradation, *J. Colloid Interface Sci.* 476 (2016) 193–199.
- [35] K. Wang, Q. Li, B. Liu, B. Cheng, W. Ho, J. Yu, Sulfur-doped g-C<sub>3</sub>N<sub>4</sub> with enhanced photocatalytic CO<sub>2</sub>-reduction performance, *Appl. Catal. B* 176–177 (2015) 44–52.
- [36] N. Sagara, S. Kamimura, T. Tsubota, T. Ohno, Photoelectrochemical CO<sub>2</sub> reduction

by a p-type boron-doped g-C<sub>3</sub>N<sub>4</sub> electrode under visible light, *Appl. Catal. B* 192 (2016) 193–198.

[37] F. Junwei, Z. Bicheng, J. Chuanjia, C. Bei, Y. Wei, Y. Jiagu, Hierarchical porous O-doped g-C<sub>3</sub>N<sub>4</sub> with enhanced photocatalytic CO<sub>2</sub> reduction activity, *Small* 13 (2017) 1603938.

[38] D.K.L. Chan, J.C. Yu, Facile synthesis of carbon- and oxygen-rich graphitic carbon nitride with enhanced visible-light photocatalytic activity, *Catal. Today* 310 (2018) 26–31.

[39] V. Devthade, D. Kulhari, S.S. Umare, Role of precursors on photocatalytic behavior of graphitic carbon nitride, *Mater. Today* 5 (2018) 9203–9210.

[40] W. Jiang, Q. Ruan, J. Xie, X. Chen, Y. Zhu, J. Tang, Oxygen-doped carbon nitride aerogel: A self-supported photocatalyst for solar-to-chemical energy conversion, *Appl. Catal. B* 236 (2018) 428–435.

[41] H. Li, F. Li, Z. Wang, Y. Jiao, Y. Liu, P. Wang, X. Zhang, X. Qin, Y. Dai, B. Huang, Fabrication of carbon bridged g-C<sub>3</sub>N<sub>4</sub> through supramolecular self-assembly for enhanced photocatalytic hydrogen evolution, *Appl. Catal. B* 229 (2018) 114–120.

[42] C. Sun, H. Zhang, H. Liu, X. Zheng, W. Zou, L. Dong, L. Qi, Enhanced activity of visible-light photocatalytic H<sub>2</sub> evolution of sulfur-doped g-C<sub>3</sub>N<sub>4</sub> photocatalyst via nanoparticle metal Ni as cocatalyst, *Appl. Catal. B* 235 (2018) 66–74.

[43] H. Wang, Y. Bian, J. Hu, L. Dai, Highly crystalline sulfur-doped carbon nitride as photocatalyst for efficient visible-light hydrogen generation, *Appl. Catal. B* 238 (2018) 592–598.

[44] J. Zhang, G. Zhang, X. Chen, S. Lin, L. Möhlmann, G. Dolega, G. Lipner, M. Antonietti, S. Blechert, X. Wang, Co-monomer control of carbon nitride semiconductors to optimize hydrogen evolution with visible light, *Angew. Chem. Int. Ed.* 51 (2012) 3183–3187.

[45] J. Sun, J. Zhang, M. Zhang, M. Antonietti, X. Fu, X. Wang, Bioinspired hollow semiconductor nanospheres as photosynthetic nanoparticles, *Nat. Commun.* 3 (2012) 1139.

[46] Z. Lin, X. Wang, Nanostructure engineering and doping of conjugated carbon nitride semiconductors for hydrogen photosynthesis, *Angew. Chem. Int. Ed.* 52 (2013) 1735–1738.

[47] J. Zhang, M. Zhang, R.-Q. Sun, X. Wang, A facile band alignment of polymeric carbon nitride semiconductors to construct isotype heterojunctions, *Angew. Chem. Int. Ed.* 51 (2012) 10145–10149.

[48] A. Savateev, B. Kurpil, A. Mishchenko, G. Zhang, M. Antonietti, A “waiting” carbon nitride radical anion: a charge storage material and key intermediate in direct C–H thiolation of methylarenes using elemental sulfur as the “S”-source, *Chem. Sci.* 9 (2018) 3584–3591.

[49] L. Yang, J. Huang, L. Shi, L. Cao, Q. Yu, Y. Jie, J. Fei, H. Ouyang, J. Ye, A surface modification resultant thermally oxidized porous g-C<sub>3</sub>N<sub>4</sub> with enhanced photocatalytic hydrogen production, *Appl. Catal. B* 204 (2017) 335–345.

[50] L. Ming, H. Yue, L. Xu, F. Chen, Hydrothermal synthesis of oxidized g-C<sub>3</sub>N<sub>4</sub> and its regulation of photocatalytic activity, *J. Mater. Chem. A* 2 (2014) 19145–19149.

[51] G. Dong, Z. Ai, L. Zhang, Efficient anoxic pollutant removal with oxygen functionalized graphitic carbon nitride under visible light, *RSC Adv.* 4 (2014) 5553–5560.

[52] J. Liu, W. Li, L. Duan, X. Li, L. Ji, Z. Geng, K. Huang, L. Lu, L. Zhou, Z. Liu, W. Chen, L. Liu, S. Feng, Y. Zhang, A graphene-like oxygenated carbon nitride material for improved cycle-life lithium/sulfur batteries, *Nano Lett.* 15 (2015) 5137–5142.

[53] S. Liu, D. Li, H. Sun, H.M. Ang, M.O. Tadé, S. Wang, Oxygen functional groups in graphitic carbon nitride for enhanced photocatalysis, *J. Colloid Interface Sci.* 468 (2016) 176–182.

[54] X. She, J. Wu, J. Zhong, H. Xu, Y. Yang, R. Vajtai, J. Lou, Y. Liu, D. Du, H. Li, P.M. Ajayan, Oxygenated monolayer carbon nitride for excellent photocatalytic hydrogen evolution and external quantum efficiency, *Nano Energy* 27 (2016) 138–146.

[55] W. Chao, F. Huiqing, R. Xiaohu, M. Jiangwei, F. Jiawen, W. Weijia, Hydrothermally induced oxygen doping of graphitic carbon nitride with a highly ordered architecture and enhanced photocatalytic activity, *ChemSusChem* 11 (2018) 700–708.

[56] J.-W. Zhang, S. Gong, N. Mahmood, L. Pan, X. Zhang, J.-J. Zou, Oxygen-doped nanoporous carbon nitride via water-based homogeneous supramolecular assembly for photocatalytic hydrogen evolution, *Appl. Catal. B* 221 (2018) 9–16.

[57] F. Wei, Y. Liu, H. Zhao, X. Ren, J. Liu, T. Hasan, L. Chen, Y. Li, B.-L. Su, Oxygen self-doped g-C<sub>3</sub>N<sub>4</sub> with tunable electronic band structure for unprecedentedly enhanced photocatalytic performance, *Nanoscale* 10 (2018) 4515–4522.

[58] Y. Wang, M.K. Bayazit, S.J.A. Moniz, Q. Ruan, C.C. Lau, N. Martsinovich, J. Tang, Linker-controlled polymeric photocatalyst for highly efficient hydrogen evolution from water, *Energy Environ. Sci.* 10 (2017) 1643–1651.

[59] D.R. Miller, D.C. Swenson, E.G. Gillan, Synthesis and structure of 2,5,8-Triazido-s-Heptazine: an energetic and luminescent precursor to nitrogen-rich carbon nitrides, *J. Am. Chem. Soc.* 126 (2004) 5372–5373.

[60] V.W.-h. Lau, I. Moudrakovski, T. Botari, S. Weinberger, M.B. Mesch, V. Duppel, J. Senker, V. Blum, B.V. Lotsch, Rational design of carbon nitride photocatalysts by identification of cyanamide defects as catalytically relevant sites, *Nat. Commun.* 7 (2016) 12165.

[61] J. Chen, X. Xu, T. Li, K. Pandiselvi, J. Wang, Toward high performance 2D/2D hybrid photocatalyst by electrostatic assembly of rationally modified carbon nitride on reduced graphene oxide, *Sci. Rep.* 6 (2016) 37318.

[62] N. Meng, J. Ren, Y. Liu, Y. Huang, T. Petit, B. Zhang, Engineering oxygen-containing and amino groups into two-dimensional atomically-thin porous polymeric carbon nitrogen for enhanced photocatalytic hydrogen production, *Energy Environ. Sci.* 11 (2018) 566–571.

[63] S. Sun, W. Wang, D. Li, L. Zhang, D. Jiang, Solar Light driven pure water splitting on quantum sized BiVO<sub>4</sub> without any cocatalyst, *ACS Catal.* 4 (2014) 3498–3503.